

Thermodynamic Properties of Single Ion Channel Formation: Gramicidin

Ryan W. Davis,[†] Elizabeth L. Patrick,[‡] Lauren A. Meyer,[†] Theodore P. Ortiz,[†]
Jason A. Marshall,[†] David J. Keller,[†] Susan M. Brozik,^{*,‡} and James A. Brozik^{*,†}

Department of Chemistry, The University of New Mexico, Albuquerque, New Mexico 87131, and Microsensor Science and Technology, Sandia National Laboratories, Albuquerque, New Mexico 87185-0892

Received: January 21, 2004; In Final Form: July 2, 2004

Single molecule fluorescence imaging has been used to unequivocally differentiate between rhodamine-6G labeled gramicidin monomeric subunits and channel-forming dimers. Absolute identification of individual particles was achieved by accounting for both particle diffusion and intensity, with dimer intensity being twice that of the monomers. In accordance with current diffusion models of proteins in bilayer membranes, we observed dimers to diffuse more slowly through the bilayer than the monomers and have reported diffusion coefficients of 1.2×10^{-8} and 3.5×10^{-8} cm²/s for the dimers and monomers, respectively. By correlating the diffusion data with measured fluorescence intensities of the tracked particles, it was possible to determine the distribution of monomers and dimers within the bilayer at various temperatures. The results allow complete characterization of the thermodynamic properties of dimer formation, $2G_1 \leftrightarrow G_2$, necessary for channel function. Reported are the temperature-dependent equilibrium constants, $\Delta H_{\text{Reaction}}^\circ$, $\Delta G_{\text{Reaction}}^\circ$, and $\Delta S_{\text{Reaction}}^\circ$, for dimer formation in an artificial lipid membrane that has a thickness (30 Å) which is on the same order as the length of the gramicidin channel (26 Å). These experiments compliment and expand single molecule fluorescence methods needed to understand the complexities of ion channel structure/function relationships.

I. Introduction

The identification of specific structural states and the statistical distribution of different structural states of membrane bound proteins in near-native conditions can profoundly affect our understanding of the structural, kinetic, and thermodynamic principles that govern their function. Gramicidin is a 15 amino acid peptide that forms a β -helix in a lipid bilayer.^{1–3} Membrane channels can only form after two monomer subunits (G_1) come together to form a head-to-head dimer (G_2) at their N-termini, stabilized by six hydrogen bonds at their dimer junction.^{1,2,4} Transmembrane pores that result from dimer formation have been shown to be 26 Å long and 4 Å in diameter and have a hydrophobic length of ~ 22 Å.^{5–7} Combined fluorescence and electrochemical experiments have shown that the majority of dimers will lead to a channel-forming pore that spans the lipid membrane⁸ and allows for an ion flux of 10^6 – 10^7 ions/s (monovalent cations; for applied potentials between 150 and 200 mV).^{1–3,9} The gramicidin channel embedded in synthetic lipid bilayer membranes serves as a model system for understanding the basic characteristics of ion channel structure/function relationships and has been the subject of extensive experimental and theoretical studies.^{3–8,10–16} Recently, experiments that combine single molecule fluorescence detection to probe structure and single channel electrical recordings to probe function have suggested subtle structure/function relationships that cannot be observed in the bulk due to ensemble averaging including multiple conformations in the open and closed states within a lipid bilayer.^{17,18} These studies point to the importance of single molecule methods for developing a better understand-

ing of structure/function relationships for membrane bound proteins in general and ion channels in particular.

A necessary condition for channel opening is dimer formation, and the simplest mechanism for closing a channel is by dimer disassociation. Therefore the functionally important process of channel formation is mainly controlled by the equilibrium constant:

$$2G_1 \leftrightarrow G_2$$

$$K_{\text{eq}}^{\text{SD}} = \frac{(SD_{G_2}/SD^\circ)}{(SD_{G_1}/SD^\circ)^2} \quad (1)$$

where SD_{G_2} is the surface density of the dimer, SD_{G_1} is the surface density of the monomer, and SD° is the standard molar surface density ($SD^\circ = 1 \text{ mol/cm}^2$). The reported equilibrium constants range from 10^{11} to $>10^{14}$.^{8,19} This large range of values depends largely upon the thickness of the lipid bilayer, but the nature of the bilayer membrane, salt concentration of the surrounding solution, membrane voltage, and cholesterol concentration also play a smaller role on the equilibrium constant.^{6–8,14,15} Much of the function of gramicidin ion channels also depends on their diffusion through and across lipid bilayer membranes. These diffusion rates can vary greatly depending on the temperature (large changes at phase transitions), concentration of cholesterol in the lipid bilayer, and the size of the particle diffusing through the membrane.^{14,17,20}

In this study we report the thermodynamics and diffusion properties of gramicidin using single molecule fluorescence imaging at several temperature points. The experimental goal is to unequivocally distinguish between individual monomers and dimers and so accurately measure their distributions at various temperatures. After determining the monomer/dimer distribution, it is straightforward to find the temperature

* To whom correspondence should be addressed. E-mail: J.A.B., brozik@unm.edu; S.M.B., smbrozik@sandia.gov.

[†] The University of New Mexico.

[‡] Sandia National Laboratories.

dependence of the equilibrium constant ($K_{\text{eq}}^{\text{Conc}}$), the standard Gibbs free energy of reaction ($\Delta G_{\text{Reaction}}^{\circ}$), the standard enthalpy of reaction ($\Delta H_{\text{Reaction}}^{\circ}$), the standard entropy of reaction ($\Delta S_{\text{Reaction}}^{\circ}$), and diffusion constants of dimers and monomers.

II. Experimental Section

(A) Gramicidin Labeling/Materials and Supplies. Literature methods were used to label the gramicidin subunits with Rhodamine-6G on their hydrophilic ends.²¹ The labeled gramicidin was then purified with a Sephadex LH-20 size exclusion column (Amersham Biosciences). All organic solvents were reagent grade, purchased from EM Science, and used as received. Gramicidin D (isolated from *Bacillus brevis*; 80–85% gramicidin A, 6–7% B, and 5–14% C), triethylamine (TEA), cholesterol, and dihexadecyldimethylammonium bromide (DHADAB) were purchased from Aldrich Chemical Co. (5/6)-carboxyrhodamine-6G-(C₆H₁₂)-NHS ester was purchased from Molecular Probes Inc. and dimyristoyl-*syn*-glycero-phosphocholine (DMPC) was purchased from Avanti Polar Lipids Inc.

(B) Reconstitution and Bilayer Formation. Gramicidin was reconstituted into lipid vesicles according to Gritsch et al.²² The lipid cake containing labeled gramicidin and 35 mol % cholesterol was formed by adding 3.08 mg of DMPC, 1.16 mg of cholesterol, 0.57 mg of DHADAB, and 8.0×10^{-12} mg of labeled gramicidin (a 7.0 μL aliquot of a 5×10^{-7} M stock methanolic solution) to 4 mL of CHCl₃. The solution was spun in a round-bottom flask at 100 rpm for 25 min to homogenize the mixture, followed by rotary evaporation to form the lipid cake, and then overnight vacuum desiccation. Lipid vesicles were reconstituted from the cake by adding 4 mL of 10 mM Tris buffer (pH 7.4) and spinning at 75 rpm and 65 °C in a round-bottom flask for 30 min. The temperature was then decreased to 45 °C and the mixture spun for 2 h. Finally, the temperature was increased to 60 °C and spun for an additional 45 min. The reconstituted vesicles were then cycled through five consecutive freeze–thaw cycles (–198 to +50 °C), followed by vesicle extrusion with a mini-extruder (Avanti Polar Lipids Inc.) equipped with a 0.4 μm pore diameter polycarbonate membrane. The final labeled gramicidin concentrations were verified by UV–vis spectroscopy from a standard calibration curve derived from known concentrations of rhodamine-6G.

Samples for single molecule particle tracking experiments were prepared on high index of refraction (1.78) flint glass coverslips (Olympus Inc.), cleaned with concentrated sulfuric acid followed by extensive rinsing with Nanopure (18 G Ω) water, dried under a stream of dry nitrogen, and UV-ozonated for 30 min prior to use. Gramicidin incorporated lipid bilayers were formed on the prepared flint glass substrates by the vesicle adsorption/collapse technique described by Brian and McConnell and characterized by Leonenko et al.^{23,24} Assuming 100% incorporation of gramicidin into the membrane²⁵ and using the facts that each lipid molecule occupies a 0.6 nm² area at the surface of the membrane^{26,27} and that the lipid bilayer is 3 nm thick (measured by ellipsometry; Gaertner L116SF/Gaertner Scientific Corp.; this is a measure of the headgroup to headgroup bilayer thickness.), the total concentration of gramicidin subunits, [G₀], in the membrane is calculated to be 1.17 μM , with a total surface density of 3.50×10^{-16} mol/cm² in the present study. The hydrophobic region of the lipid bilayer used in this study was previously measured using electrical impedance spectrometry and found to be 2.8 nm.^{28,29}

(C) Single Molecule Fluorescence Microscopy and Temperature Control. The microscope used in the single molecule fluorescence studies is depicted in Figure 1. In this apparatus

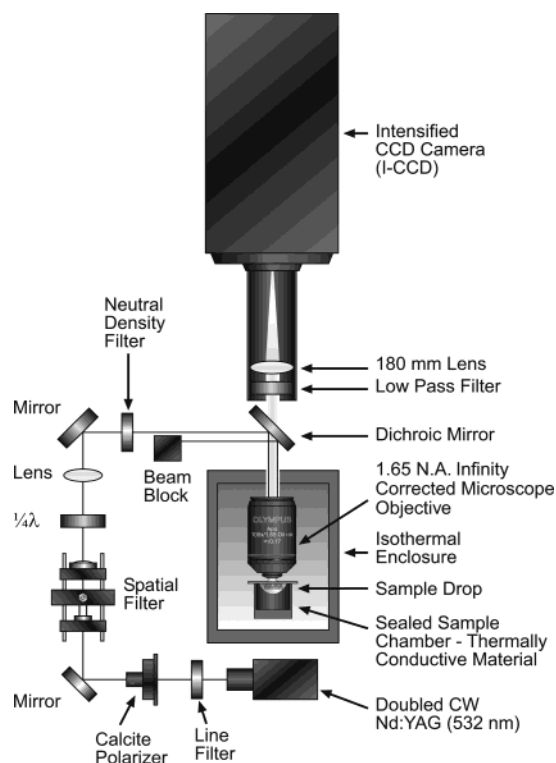


Figure 1. Microscope configuration. The 532 nm excitation was produced by a Nd:YAG laser and attenuated to ~ 1 mW. Single molecule fluorescence collected by a 1.65 NA infinity corrected microscope objective. Single molecule images collected with an ICCD camera operating at a 100 ms frame rate.

the beam from a doubled cw-Nd:YAG laser (532 nm, 10 mW, BWTEK Inc.) is passed through a 532 nm laser line filter (± 2 nm fwhm, OptoSigma Corp.), a calcite polarizer, and a $1/4$ waveplate to produce a clean circularly polarized beam. The beam is then passed through a spatial filter, attenuated to 1 mW with a neutral density filter, and focused on the back of the microscope objective with a 500 mm focal length quartz lens. The focused beam is directed onto the edge of a 1.65 NA infinity corrected microscope objective (Olympus Inc.) with a dichroic mirror (QS4SLP, Chroma Technologies Corp.) such that the deflected beam is totally internally reflected at the flint glass/water interface. Figure 2 shows the orientation of the exciting evanescent field to the sample incorporated within the lipid bilayer. The size of the laser beam at the glass/water interface was 6 μm^2 . Fluorescence from a single labeled gramicidin monomer or dimer was collected through the microscope objective, passing through the dichroic mirror, filtered with a long pass filter (HQ550LP, Chroma Technologies Corp.) to remove scattered laser light, and imaged on an intensified CCD camera (IPentaMax, Roper Scientific Inc.) with a quartz lens. Fluorescence from single molecules yielded diffraction limited spots (~ 250 nm) that covered a 6×6 area of pixels on the ICCD camera (fwhm).

The sample was inverted relative to the flint glass cover slip and sealed around a chamber with thermally conducting walls to prevent evaporation and maintain thermal equilibrium with the isothermal enclosure that surrounded the sample. The temperature within the isothermal enclosure was set and maintained with a combination of a thermostat and a ceramic heating element. The temperature within the isothermal enclosure was measured with a J-type thermocouple mounted in near contact with the sample. For the temperature-dependent experi-

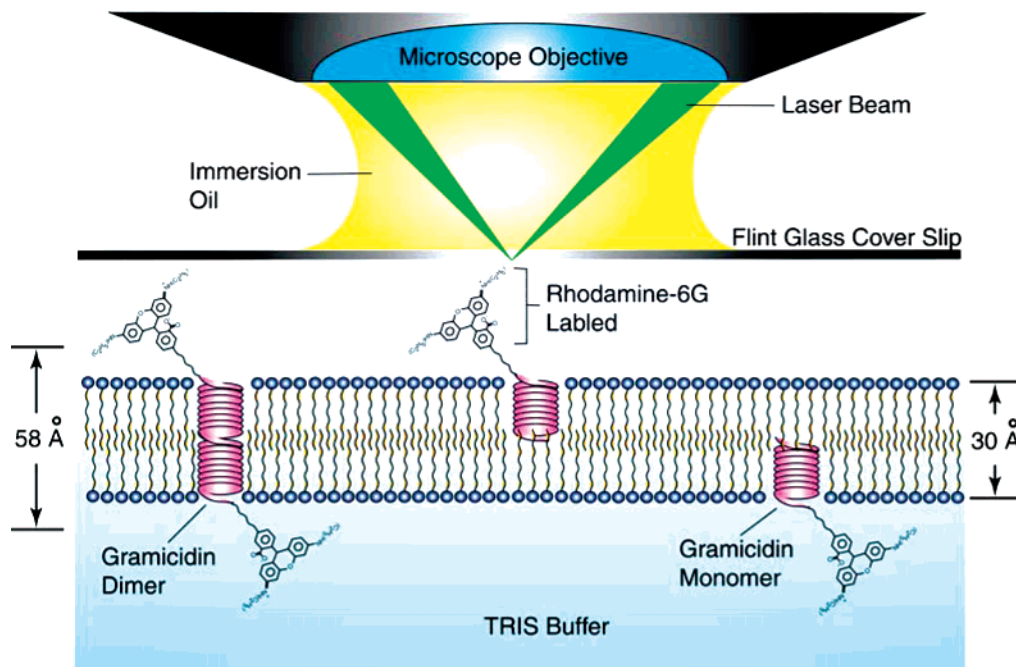


Figure 2. Optical orientation of sample relative to the evanescent field held as an inverted droplet. The lipid bilayer membrane is ~ 30 Å thick, and opposing fluorescent tags are separated by ~ 58 Å.

ments the concentration was fixed at $1.17 \mu\text{M}$ and the temperature changed from 21.5 to 33.2 °C in seven nearly equal steps.

(D) Diffusion/Particle Tracking/Intensity Analysis. Image recording and single molecule tracking was aided by the WinView software package supplied by Roper Scientific in tandem with a custom-made C program. Individual mean-square displacements were based upon

$$\bar{r}^2(t) = \left(\frac{1}{N-1} \right) \sum_{t=t_0}^t |r(t) - r(t-t_0)|^2 \quad (2)$$

where $\bar{r}^2(t)$ is the mean square displacement, $r(t)$ is the position vector at time t , N is the total number of frames, and $t_0 = 0.1$ s is the frame rate from the data acquisition. The lateral diffusion constant (D) is then related to the mean square displacement by

$$\bar{r}^2(t) = 4Dt \quad (3)$$

From eq 3, the diffusion constant of individual particles was determined by plotting \bar{r}^2 vs time for the entire trajectory of tracked single particles. The lateral diffusion coefficients of each particle were then determined from the slope of these lines.

The average intensity for each tracked particle was derived from the Gaussian fluorescence peak of the individual particles in each frame. The reported intensity is the average over such peak intensities in all frames for the individual particles.

III. Results and Discussion

(A) Thermodynamic Analysis from Single Molecule Data.

The thermodynamic properties were determined from the measured distribution of monomers vs dimers within the lipid membrane. The equilibrium constant for dimer formation, expressed in terms of molar concentrations, is

$$K_{\text{eq}}^{\text{Conc}} = \frac{([G_2]/C^\circ)}{([G_1]/C^\circ)^2} \quad (4)$$

where $C^\circ = 1 \text{ mol/L}$ is the standard molar concentration. The fractional populations of the monomers and dimers are defined as

$$f(G_1) = \frac{\text{number of } G_1 \text{'s counted}}{\text{total number of particles counted}} \quad (5)$$

$$f(G_2) = \frac{\text{number of } G_2 \text{'s counted}}{\text{total number of particles counted}} \quad (6)$$

If $[G_0]$ is the total concentration of gramicidin subunits, then

$$f(G_2) = \frac{[G_2]}{[G_0] - [G_2]} \quad (7)$$

and

$$[G_2] = \frac{f(G_2)[G_0]}{(1 + f(G_2))} \quad (8)$$

$$[G_1] = [G_0] - 2[G_2] \quad (9)$$

Therefore equilibrium constants can be determined from single molecule fluorescence data by identifying and counting single particles.

The standard enthalpy of reaction, $\Delta H_{\text{Reaction}}^\circ$, can then be determined by measuring the temperature dependence of the equilibrium constant over a small, but reasonable, temperature range, using the van't Hoff equation

$$\ln \left(\frac{K_{\text{eq}}^{\text{Conc}}(T_2)}{K_{\text{eq}}^{\text{Conc}}(T_1)} \right) = \frac{-\Delta H_{\text{Reaction}}^\circ}{R} \left(\frac{1}{T_2} - \frac{1}{T_1} \right) \quad (10)$$

and the entropy of reaction can be found from

$$\Delta G_{\text{Reaction}}^\circ(T) = -R(T) \ln K(T) = \Delta H_{\text{Reaction}}^\circ(T) - T\Delta S_{\text{Reaction}}^\circ(T) \quad (11)$$

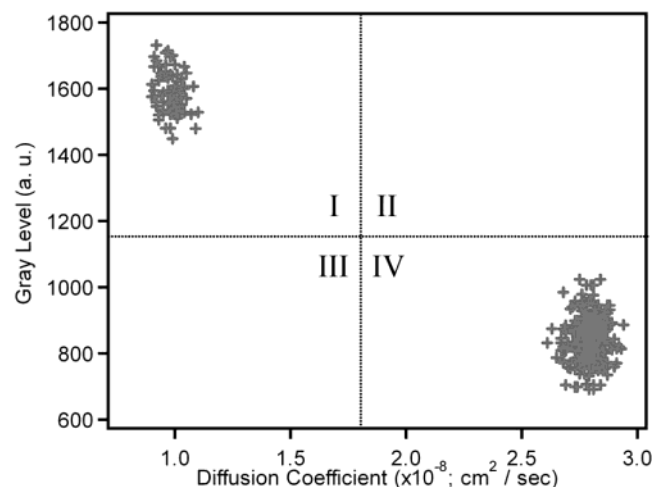


Figure 3. Scatter plot of raw intensity from ICCD camera (in arbitrary gray scale) vs measured diffusion coefficient within the membrane. Experiment performed at 21.5 °C.

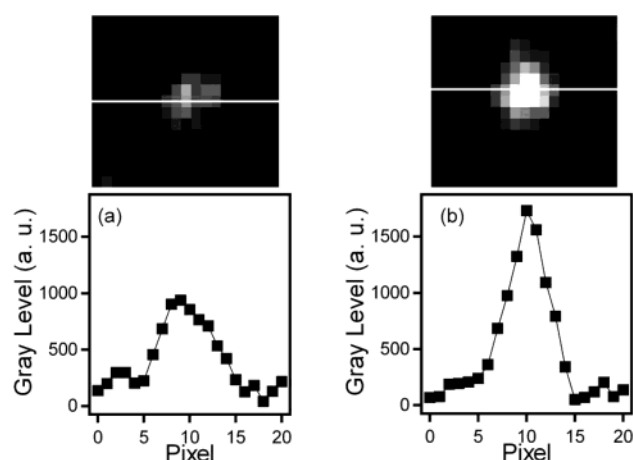


Figure 4. Intensity slice of single molecule fluorescence images: (a) typical monomer image; (b) typical dimer image. Frames integrated for 100 ms.

(B) Identifying and Sampling Gramicidin Monomers and Dimers. Gramicidin dimers can be clearly distinguished from gramicidin monomers by both fluorescence intensity and diffusion coefficient. Figure 3 shows clear, well-separated clusters, and high correlation between brightness and diffusion coefficient: dim particles diffuse fast, bright particles diffuse more slowly, as expected if the dim particles are monomers and the bright particles are dimers. Furthermore, two-step photobleaching and photoblinking has been observed for a small number of particles that fall into region I of Figure 3, providing additional evidence that the bright, slow diffusing particles are dimers. No two-step photobleaching or photoblinking was observed for particles that fall into region IV of Figure 3. As shown in Figure 4, bright particles are almost twice as intense as dim particles, again consistent with their identity as dimers. It should be noted that because a dimer is nearly 30 Å in length and the hydrocarbon linker attached to the fluorescent tag is an additional 14 Å, then the fluorescent tags are separated by up to 58 Å, much longer than the Förster radius for rhodamine-6G pairs (Förster radius \approx 20 Å). Self-quenching of opposing dyes should thus be minimal. It is known, through Stokes–Einstein’s law of diffusion, that particles with larger sizes will move more slowly through a viscous medium than particles with smaller sizes because of their increased drag. A lipid bilayer is not an isotropic medium but is rather anisotropic and gramicidin dimers

TABLE 1: Temperature-Dependent Equilibrium Constants,^{a,b} Average Diffusion, and Relative Intensities

temp (°C)	$10^{-5}K_{\text{eq}}^{\text{Conc}}(T)$	$10^8 D_{G_1}$ (cm ² /s)	$10^8 D_{G_2}$ (cm ² /s)	G_1 intensity (gray level, au) ^c	G_2 intensity (gray level, au) ^c
21.5	2.70	2.8 ± 0.1	0.96 ± 0.05	830	1589
22.7	2.51	3.5 ± 0.1	1.2 ± 0.09	951	1774
25.4	2.12	3.5 ± 0.1	1.2 ± 0.1	942	1912
26.7	1.81	3.6 ± 0.1	1.2 ± 0.09	890	1746
28.2	1.57	3.7 ± 0.1	1.1 ± 0.1	944	1834
31.0	1.31	3.8 ± 0.1	1.1 ± 0.1	895	1698
33.2	1.26	4.1 ± 0.1	1.2 ± 0.1	921	1779

^a Total membrane concentration = $[G_0] = [G_1] + 2[G_2] = 1.17 \times 10^{-6}$ M. ^b $K_{\text{eq}}^{\text{Conc}}$ given by eq 4. ^c Gray level depends on intensifier gain setting. Different temperature points were taken on separate days and the intensifier was optimized each day, which leads to slightly different gray levels between temperature points.

are more like cylinders than spheres. Therefore one would not expect the diffusivity to have an exactly inverse relationship to the size of the particle, but the inverse trend will hold approximately.^{20,30–33} The measured diffusion coefficients at 25 °C are 1.2×10^{-8} and 3.5×10^{-8} cm²/s for the dimer and monomer, respectively (diffusion coefficients are summarized in Table 1). It should also be noted that the particles that diffuse quickly, identified as gramicidin monomers, have a near Gaussian distribution. This effectively eliminates the possibility that the bilayer leaflet in closest proximity to the flint glass substrate is significantly less mobile than the opposing leaflet. If the mobility of the two leaflets were significantly different, one would expect two separate and distinct distributions for monomer particles. Using fluorescence recovery after photobleaching, Tank et al. reported diffusion constants for the gramicidin dimer embedded in DMPC lipid bilayers and recorded at a variety of temperatures and cholesterol concentrations. At 35 mol % of cholesterol and 25 °C, they reported a diffusion constant of $\sim 1 \times 10^{-8}$ cm²/s, which is very close to our measured value under similar sample conditions.¹⁴ Furthermore, our reported monomer diffusion is also in agreement with that measured by Borisenko et al. from a previous single molecule study (3.3×10^{-8} cm²/s) in a lipid bilayer composed of dioleoylphosphatidylcholine.¹⁷ Although measuring either the relative fluorescence intensities or the diffusivity is good for identifying the particles, it becomes a much more convincing argument if the two measurements can be correlated. Such a correlation is displayed in Figure 3 and the bimodal distribution of the fluorescence intensity with particle diffusivity allows one to unequivocally categorize the particles as either monomers or dimers. Hence, the particles that fall into region I are dimers and those in region IV are monomers (Figure 3). From this distribution the equilibrium constants can be determined as described in the preceding section. The measured equilibrium constants are collected in Table 1.

(C) Temperature Dependence. Depicted in Figure 5 is a plot of $\ln(K_{\text{eq}}^{\text{Conc}})$ vs $1/T$ from experimental equilibrium constant data (the circles). From the slope, $\Delta H_{\text{Reaction}}^{\circ} = -53.0$ kJ/mol; the formation of the dimer is thus an exothermic process, as expected. Moreover, because the energy of a typical hydrogen bond is between 8 and 10 kJ/mol, the measured $-\Delta H_{\text{Reaction}}^{\circ}$ is consistent with the model proposed by Urry et al. in which the dimer involves the formation of six hydrogen bonds.¹⁴ The value of $\Delta H_{\text{Reaction}}^{\circ}$ compliments the results of Bamberg and Lauger who determined that the formation of a gramicidin dimer embedded in a 50 Å thick lipid matrix was an endothermic process with $\Delta H_{\text{Reaction}}^{\circ} = +13.4$ kJ/mol.³⁴ In that earlier study, the authors concluded that, because the membrane was considerably thicker than a gramicidin dimer, the energy liberated by

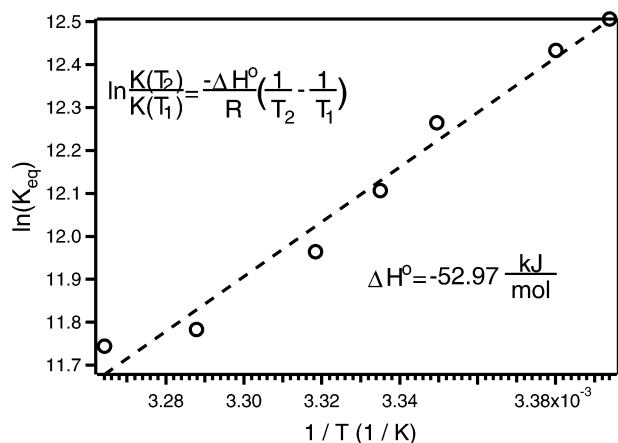


Figure 5. Plot of $\ln(K_{eq}^{Conc})$ vs $1/T$. Circles are the experimental data, and the dashed line is a linear fit of the data to the van't Hoff equation (eq 10).

the formation of six hydrogen bonds (an exothermic process) was more than compensated by the energy required to distort the lipid matrix (an endothermic process). Thus making the overall process endothermic. In the present study, the lipid thickness (30 Å) and the length of the dimer (26 Å) are approximately matched. Moreover, the length of the hydrophobic region (22 Å)^{6,7} of the gramicidin dimers also approximately matches the hydrophobic region of the lipid bilayer (28 Å),^{28,29} so one would not expect such a severe distortion of the lipid matrix upon dimer formation. The measured $\Delta H_{Reaction}^{\circ}$ in the current study should therefore more closely reflect the intrinsic enthalpy of dimer formation irrespective of the lipid bilayer. The measured $K_{eq}^{SD}(25^{\circ}\text{C})$ value agrees with the observations made by Veatch et al. over 20 years ago when they observed that $K_{eq}^{SD}(25^{\circ}\text{C}) \geq 10^{14}$ for a membrane that was 31 Å thick.⁸ From the measured equilibrium constant, $\Delta G_{Reaction}^{\circ}$ has a value of -30.4 kJ/mol. Finally, from $\Delta H_{Reaction}^{\circ}$ and $\Delta G_{Reaction}^{\circ}$, $\Delta S_{Reaction}^{\circ}$ has a value of -75.8 J/mol K. Assuming that the major contribution to $\Delta S_{Reaction}^{\circ}$ is associated with the translational degrees of freedom ($\Delta S_{Reaction}^{\circ} \approx \Delta S_{Reaction,trans}^{\circ}$), one can estimate $\Delta S_{Reaction}^{\circ}$ from pure translational partition functions for monomers and dimers:³⁵

$$\Delta S_{Reaction,trans}^{\circ} = k \ln \left(\frac{2t}{e} \Lambda_{G_1}^2 C_{3D}^{\circ} \right) \quad (12)$$

where k is Boltzmann's constant, t is the thickness of the membrane, $\Lambda_{G_1}^2 = (h^2/2\pi mkT)$, m is the mass of a gramicidin monomer, and C_{3D}° is the standard molar concentration in units of molecules/m³. With $t = 3$ nm, $m = 3.13 \times 10^{-24}$ kg, and $C_{3D}^{\circ} = 1M = 6.02 \times 10^{26}$ molecules/m³, eq 12 yields $\Delta S_{Reaction,trans}^{\circ} = -98.4$ J/(mol K). The close correlation between measured and calculated values suggests that the negative change in standard entropy of reaction is primarily due to the loss of translational freedom upon dimerization and the different masses of monomers vs dimers, with only minor contributions from the lipid membrane and other degrees of freedom associated with the products and reactants. The thermodynamic data are collected in Table 2.

IV. Summary

Without question gramicidin in artificial lipid bilayers has become the most important model system for the study of membrane bound ion channels in biological systems and has been the subject of intense study for at least 30 years. In that time there have been many well-formulated studies involving

TABLE 2: Standard Thermodynamic Quantities of Reaction at 25 °C for $2G_1 \leftrightarrow G_2$

ΔH° (kJ/mol)	K_{eq}^{Conc} ($T = 25^{\circ}\text{C}$)	K_{eq}^{SD} ($T = 25^{\circ}\text{C}$) ^{a,b}	ΔG° (kJ/mol)	ΔS° (J/mol K)
-53.0	2.09×10^5	6.86×10^{14}	-30.4	-75.8

^a Total surface density = $SD_{G_0} = SD_{G_1} + 2SD_{G_2} = 3.50 \times 10^{-16}$ mol/cm². ^b K_{eq}^{SD} given by eq 1.

single channel electrical recordings and ensemble spectroscopic measurements (NMR and fluorescence). These studies have been used to elucidate structure, function, rates of channel formation, ion flux, the thermodynamic properties of the transition state, etc. Even so, the basic thermodynamic properties (standard enthalpy, Gibbs free energy, and entropy of reaction) have never been measured. This is due in part to the large equilibrium constant for dimer formation (the chemical reaction responsible for "turning on" the ion channel) and the lack of the necessary tools needed to directly measure the equilibrium constant. In this study we have directly measured the standard free energy of reaction and the standard enthalpy of reaction using single molecule fluorescence techniques to unequivocally distinguish monomers from dimers and hence have directly measured their absolute distribution in a lipid bilayer at different temperatures. In addition, this work has made use of rigorous thermodynamic arguments to augment the experimental results. In short, the study presented above uses new state of the art fluorescence techniques to address a fundamental problem in an important model system.

Acknowledgment. We acknowledge grants from NIH (GM63808), NSF(IGERT), and Sandia National Laboratories for partial support of this research. Sandia is a multiprogram laboratory operated by Sandia Corp., a Lockheed Martin company, for the United States Department of Energy's National Nuclear Security Administration under Contract DE-AC04-94AL85000. The University of New Mexico and Sandia National Laboratories are also thanked for programmatic support.

References and Notes

- (1) Koeppe, R. E., II; Andersen, O. S. *Annu. Rev. Biophys. Biomol. Struct.* **1996**, 25, 231.
- (2) Woolley, G. A.; Wallace, B. A. *J. Membr. Biol.* **1992**, 129, 109.
- (3) Anderson, O. S.; Apell, H. J.; Bamberg, E.; Busath, D. D.; Koeppe, R. E., II; Sigworth, F. J.; Szabo, G.; Urry, D. W.; Woolley, G. A. *Nature Struct. Biol.* **1999**.
- (4) Urry, D. W.; Goodall, M. C.; Glickson, J. D.; Mayers, D. F. *Proc. Natl. Acad. Sci. U.S.A.* **1971**, 68, 1907.
- (5) Urry, D. W. *Proc. Natl. Acad. Sci. U.S.A.* **1971**, 68, 672.
- (6) Elliott, J. R.; Needham, D.; Dilger, J. P.; Haydon, D. A. *Biochem. Biophys. Acta* **1983**, 735, 95.
- (7) Huang, H. W. *Biophys. J.* **1986**, 50, 1061.
- (8) Veatch, W. R.; Mathies, R.; Eisenberg, M.; Stryer, L. *J. Mol. Biol.* **1975**, 99, 75.
- (9) O'Connell, A. M.; Koeppe, R. E., II; Andersen, O. S. *Science* **1990**, 250, 1256.
- (10) Bamberg, E.; Apell, H. J.; Alpes, H. *Proc. Natl. Acad. Sci. U.S.A.* **1977**, 74, 2402.
- (11) Bamberg, E.; Apell, H. J.; Alpes, H.; Gross, E.; Morell, J. L.; Harbaugh, J. F.; Janko, K.; Lauger, P. *Federation Proc.* **1978**, 37, 2633.
- (12) Szabo, G.; Urry, D. W. *Science* **1979**, 203, 55.
- (13) Weinstein, S.; Wallace, B. A.; Blout, E. R.; Morrow, J. S.; Veatch, W. R. *Proc. Natl. Acad. Sci. U.S.A.* **1979**, 76, 4230.
- (14) Tank, D. W.; Wu, E. S.; Meers, P. R.; Webb, W. W. *Biophys. J.* **1982**, 40, 129.
- (15) Schagina, L. V.; Blasko, K.; Grinfeldt, A. E.; Korchev, Y. E.; Lev, A. A. *Biochim. Biophys. Acta* **1989**, 978, 145.
- (16) Chernyshev, A.; Cukierman, S. *Biophys. J.* **2002**, 82, 182.
- (17) Borisenko, V.; Loughheed, T.; Hesse, J.; Fureder-Kitzmüller, E.; Fertig, N.; Behrends, J. C.; Woolley, G. A.; Schutz, G. J. *Biophys. J.* **2003**, 84, 612.

- (18) Harms, G. S.; Orr, G.; Montal, M.; Thrall, B. D.; Colson, S. D.; Lu, H. P. *Biophys. J.* **2003**, *85*, 1826.
- (19) Rokitskaya, T. I.; Antonenko, Y. N.; Kotova, E. A. *Biochem. Biophys. Acta* **1996**, *1275*, 221.
- (20) Saffman, P. G.; Delbruck, M. *Proc. Natl. Acad. Sci. U.S.A.* **1975**, *72*, 3111.
- (21) Loughheed, T.; Borisenko, V.; Hand, C. E.; Woolley, G. A. *Bioconjugate Chem.* **2001**, *12*, 594.
- (22) Gritsch, S.; Nollert, P.; Jaehnig, F.; Sackmann, E. *Langmuir* **1998**, *14*, 3118.
- (23) Leonenko, Z. V.; Carnini, A.; Cramb, D. T. *Biochim. Biophys. Acta* **2000**, *1509*, 131.
- (24) Brian, A. A.; McConnell, H. M. *Proc. Natl. Acad. Sci. U.S.A.* **1984**, *81*, 6159.
- (25) Bransburg-Zabary, S.; Kessel, A.; Gutman, M.; Ben-Tal, N. *Biochemistry* **2002**, *41*, 6946.
- (26) Cevc, G.; Marsh, D. *Phospholipid Bilayers*; Wiley and Sons: New York, 1987.
- (27) Nagle, J. F.; Tristram-Nagle, T. *Biochem. Biophys. Acta* **2000**, *1469*, 159.
- (28) Branch, D. W.; Brozik, S. M.; Hughes, R. C. *SAND2001-2792A* **2001**, 1.
- (29) Hughes, R. C.; Branch, D. W.; Brozik, S. M. *SAND2003-0116* **2003**, 1.
- (30) Cohen, M. H.; Turnbull, D. *J. Chem. Phys.* **1959**, *31*, 1164.
- (31) Traeuble, H.; Sackmann, E. *J. Am. Chem. Soc.* **1972**, *94*, 4499.
- (32) Galla, H. J.; Hartmann, W.; Theilen, U.; Sackmann, E. *J. Membr. Biol.* **1979**, *48*, 215.
- (33) Ke, P. C.; Naumann, C. A. *Langmuir* **2001**, *17*, 3727.
- (34) Bamberg, E.; Lauger, P. *Biochem. Biophys. Acta* **1974**, *367*, 127.
- (35) McQuarrie, D. A. *Statistical Mechanics*, 1st ed.; Harper Collins Publishers: New York, 1976.